Arabian Journal of Chemistry (2014) xxx, xxx–xxx

King Saud University

Arabian Journal of Chemistry

www.ksu.edu.sa
www.sciencedirect.com

ORIGINAL ARTICLE

CoMFA, CoMSIA, kNN MFA and docking studies of 1,2,4-oxadiazole derivatives as potent caspase-3 activators

Ankur Vaidya [a], Abhishek Kumar Jain [a], B.R. Prashantha Kumar [b], G.N. Sastry [c], Sushil Kumar Kashaw [a], Ram Kishore Agrawal [a,*]

[a] *Division of Medicinal and Computational Chemistry, Department of Pharmaceutical Sciences, Dr. H. S. Gour University, Sagar 470003, M.P., India*
[b] *JSS College of Pharmacy, Ooty, India*
[c] *Molecular Modeling Group, Organic Chemical Sciences, Indian Institute of Chemical Technology, Tarnaka, Hyderabad 500 007, India*

Received 13 August 2013; accepted 31 May 2014

KEYWORDS

Caspase;
3D-QSAR;
CoMFA;
CoMSIA;
[(SW) kNN MFA];
Docking

Abstract Caspase-3 has become an attractive target in the treatment of many diseases such as Alzheimer, Parkinson's, myocardial infarction and cancer. In the present study, molecular three-dimensional quantitative structure activity relationship (3D-QSAR) and docking studies were performed on a series of caspase-3 activators. Comparative molecular field analysis (CoMFA), comparative molecular similarity indices analysis (CoMSIA) and step-wise k-nearest neighboring molecular field analysis [(SW) kNN MFA] were performed to gain insight into the key structural factors affecting the activity. The results of 3D-QSAR are reliable and significant having high predictive (q^2) ability showing good correlation between predicted and observed activity. The lower value of standard error of estimation shows that most of the observed values cluster fairly close to the regression line. Molecular docking was performed with the GOLD docking program used to explore the binding mode between the ligands and the receptor.

1. Introduction

Cancer is a major dilemma worldwide and is the principal cause of mortality in developed countries. Nearly one in two men and more than one in three women in the United States will be diagnosed with cancer at some point in his or her life-time (Carson and Lois, 1995; Thun et al., 2006). One of the most difficult problems arising during cancer therapy is the occurrence of cancer cell invasion responsible for the spread

* Corresponding author. Tel.: +91 7582 233934; fax: +91 7582 264236.
E-mail address: shwetavaidya2000@gmail.com (R.K. Agrawal).
Peer review under responsibility of King Saud University.

Production and hosting by Elsevier

http://dx.doi.org/10.1016/j.arabjc.2014.05.034
1878-5352 © 2014 Production and hosting by Elsevier B.V. on behalf of King Saud University.

of tumor cells throughout the body (Suk et al., 2009; Sohn et al., 2010). At present, a wide range of cytotoxic drugs with different mechanisms of action are used to treat human cancer, either alone or in combination. Diverse groups of molecules are involved in the apoptosis induced cytotoxicity (Zhang et al., 2003; Silva et al., 2007). Induction of apoptosis by novel caspase substrates has become an area of intense research in oncology (Thornberry, 1998). Caspases, a group of cysteine proteases (hence the C in caspase) cleave their substrates after aspartic acid residues (hence aspase) and are the key executioners of apoptosis (Mohr and Zwacka, 2007; Syed et al., 2005). Caspases are classified into two classes i.e. initiator caspases (caspase 2, caspase 8, caspase 9 and caspase 10) and effector caspases (caspase 3, caspase 6 and caspase 7), based on the presence of a large prodomain at their amino-terminal region (Salvesen and Dixit, 1997; Marques et al., 2003; Leonard and Roy, 2006).

Caspase-3 a frequently activated death protease is the primary target for a number of anticancer agents. N-phenylnicotinamide, was first discovered as a series of novel potent apoptosis inducers that interact with tubulin (Cai et al., 2001; Dutchowicz et al., 2006). Zhang et al. (2003) reported the discovery and biological characterization of 3-aryl-5-aryl-1,2,4-oxadiazoles as a novel apoptosis inducer with tumor selective properties owing to caspase-3 activation.

Several molecular modeling aspects have been employed in the development of potent and selective caspase-3 activators. In this work, three-dimensional quantitative structure activity relationship (3D-QSAR) and molecular docking approaches were performed to study these caspase-3 activators. 3D-QSAR methods, i.e., comparative molecular field analyses (CoMFA), comparative molecular similarity indices analyses (CoMSIA) and step-wise k-nearest neighboring molecular field analysis [(SW) kNN MFA] are most valuable techniques, which involve the generation of a common three dimensional lattice around a set of molecules and calculation of interaction energies at the lattice points (Ravichandran and Agrawal, 2007; Ravichandran et al., 2007, 2008; Prashanthakumar and Nanjan 2009; V-Life). Docking studies were also performed to explore receptor-based conformation or binding pocket for each compound and consequently derived more reliable models.

2. Material and methods

2.1. Data set

A data set of thirty-two 3-aryl-5-aryl-1,2,4-oxadiazole derivatives with caspase-3 enzyme activity that induced cytotoxicity on the T47D cell line was used in the present study (Table 1) (Zhang et al., 2005a,b; Kemnitzer et al., 2009). Test and training set contained a diverse set of compounds with low, moderate and high biological activity.

2.2. Molecular structure and alignment

The 3D QSAR molecular modeling and statistical analysis were performed using the molecular modeling package SYBYL Version 6.7 (Tripos Inc., 2001) and V-Life Molecular Design Suit (MDS) software Version 3.5 using the CoMFA, CoMSIA and [(SW) kNN MFA] methods respectively. The 3D structures of all thirty-two oxadiazole compounds were built on the workspace of molecular modeling softwares SYBYL and V-Life MDS. Energy minimization was carried out using the standard tripos force field with distance dependent-dielectric function, energy gradient of 0.001 kcal/mol Å and an iteration limit of 10,000. Partial charges for all the molecules were assigned using the Gasteiger–Huckel method and they were submitted for a conformational search protocol. Bioactive conformations and molecular alignment are two imperative parameters to build more consistent 3D QSAR models. Structure alignment is considered as one of the most sensitive steps in 3D QSAR done with a template based alignment. The most active compound 10e was used as a template and each molecule was superimposed on the template via the field fit alignment (Figs. 1 and 2) (Jain et al., 2010; Vaidya et al., 2011).

2.3. Generation of CoMFA, CoMSIA and [(SW) kNN MFA] fields

After alignment molecules were placed in a common rectangular grid that extended 4 Å units beyond the aligned molecules in all directions with a grid step size of 2 Å; a probe sp^3 hybridized carbon atom with +1 charge and Van Der Waals radius of 1.52 Å was employed.

In CoMFA, steric and electrostatic field descriptors were calculated with a default cut-off of 30 kcal/mol whereas for CoMSIA all five force field properties (i.e. steric, electrostatic, hydrophobic, hydrogen-bond donor and hydrogen-bond acceptor) were determined at a 30-kcal/mol energy cut-off, which meant that energy fields greater than 30 kcal/mol are curtailed to that value, and thus can avoid infinite energy values inside the molecule.

Similar to CoMFA in the [(SW) kNN MFA] method steric and electrostatic fields were generated with a default energy of 30 kcal/mol.

2.4. Partial Least-Square (PLS) regression analysis and validation of 3D-QSAR model

Partial Least-Square (PLS) regression analysis was used to construct a linear correlation between energy fields (independent variables) with anticancer activity values (dependent variable) and cross-validation was done using the leave-one-out (LOO) method with a 2.0 kcal/mol column filter for CoMFA, CoMSIA and [(SW) kNN MFA] analyses.

The final models were validated on the basis of obtained optimum number of components (N) yielding the highest cross-validated r^2 (q^2) value with a minimum standard of error.

2.5. Molecular docking

Docking studies were employed to locate the appropriate binding orientations and conformations of these oxadiazole derivatives interacting with caspase-3 using the docking program GOLD. Gold is a fast, flexible docking method that uses an incremental construction algorithm to place ligands into an active site. By default, the docking program produces 10 docked structures for each 1,2,4-oxadiazole derivative. The conformation with the lowest docking energy in the most populated cluster is selected as the possible 'active' conformation

Please cite this article in press as: Vaidya, A. et al., CoMFA, CoMSIA, kNN MFA and docking studies of 1,2,4-oxadiazole derivatives as potent caspase-3 activators. Arabian Journal of Chemistry (2014), http://dx.doi.org/10.1016/j.arabjc.2014.05.034

Table 1 1,2,4-Oxadiazole analogs and their experimental caspase-3 activator activity

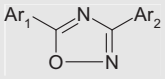

S. No.	Ar_1	Ar_2	Activity T47D (EC_{50} nM)	pIC_{50} (T47D)
1d		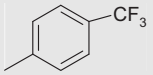	0.0012	2.9172
4a		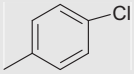	0.0018	2.7520
4b			0.0028	2.5496
4c		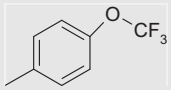	0.0009	3.0506
4d		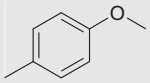	0.0042	2.3799
4e		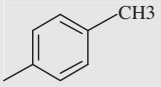	0.0037	2.4365
4g		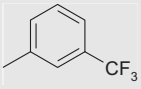	0.0009	3.0456
4h	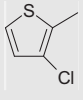	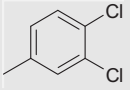	0.0014	2.8508
4i	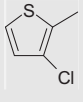	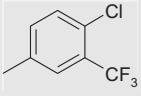	0.0009	3.0315
4j	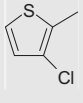	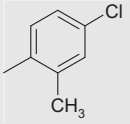	0.0009	3.0406

(*continued on next page*)

Table 1 (*continued*)

S. No.	Ar_1	Ar_2	Activity T47D (EC_{50} nM)	pIC_{50} (T47D)
4k		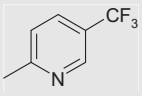	0.0014	2.8416
4l		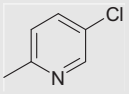	0.0016	2.7986
4m		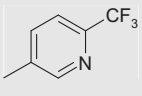	0.0009	3.0362
4n		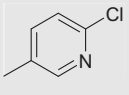	0.0008	3.1249
4o		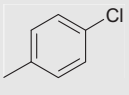	0.0033	2.4789
4v		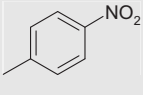	0.0020	2.7055
10a		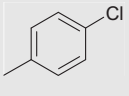	0.0011	2.9666
10b		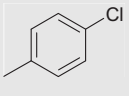	0.0017	2.7595
10c		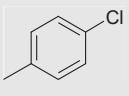	0.0174	1.7595
10d	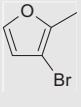	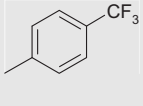	0.0020	2.6968
10e	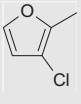	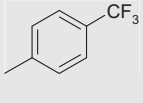	0.0005	3.2840

Table 1 (*continued*)

S. No.	Ar_1	Ar_2	Activity T47D (EC_{50} nM)	pIC_{50} (T47D)
10f		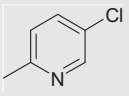	0.0016	2.7932
10g		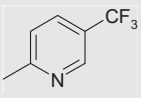	0.0006	3.2147
10h		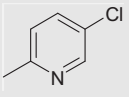	0.0011	2.9547
11a		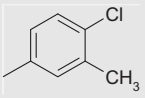	0.0017	2.7696
11b		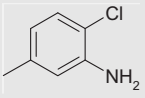	0.0024	2.6198
11c		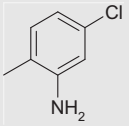	0.0031	2.5086
11d		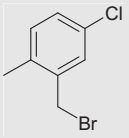	0.0045	2.3468
11e		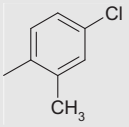	0.0011	2.9580
11f		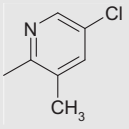	0.0009	3.0268
11g		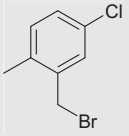	0.0022	2.6575

(*continued on next page*)

Table 1 (*continued*)

S. No.	Ar_1	Ar_2	Activity T47D (EC_{50} nM)	pIC_{50} (T47D)
11h		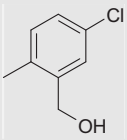	0.0029	2.5376

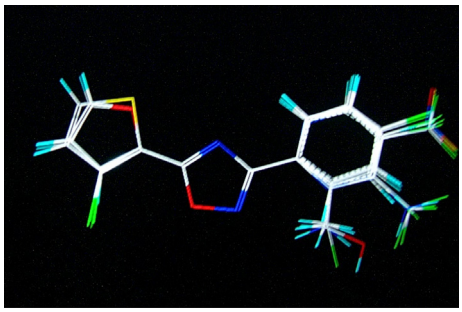

Figure 1 Field fit alignment of 1,2,4-oxadiazoles derivatives using SYBYL 6.7.

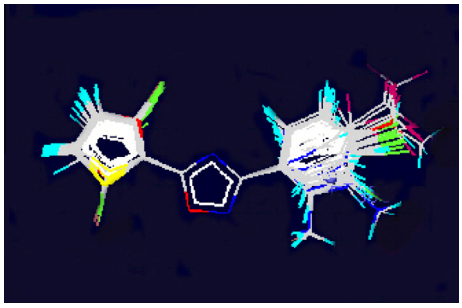

Figure 2 Field fit alignment of 1,2,4-oxadiazoles derivatives using V-Life MDS 3.5.

against the 1RE1 active site. In the present study, 32 compounds were successfully docked into the 1RE1 site.

The X-ray crystal structure of caspase-3 taken from the Protein Data Bank (pdb: 1RE1) was used to dock. At the beginning of docking, all the water molecules were removed, hydrogen atoms added and AMBER7FF99 charges to the protein were applied.

It is critical to search for the binding pocket of the prepared protein in docking studies. In Surflex-docking, the binding pockets can be defined either from a cocrystallized ligand or from a list of residues known to be part of the interacting site (or predicted de novo). The active site was defined within 5 Å surrounding to the co-crystallized ligand and the specific residues and constraints information were obtained from crystallographic data as well as an earlier study. The docking poses were ranked by Gold docking and the top ten poses were selected. The ligands were then docked inside a cubic GRID box centered at the midpoint between the Cys205 and Gly238. Ten docking runs were performed for each compound in the dataset. In most cases the chosen pose was the top-ranked solution.

3. Result and discussion

To derive 3D QSAR models, best selected model compound No. 4c, 4e, 4l, 4n, 10g and 11g were set as test set compounds, while the remaining were training set compounds.

Table 2 The comparison of 3D QSAR models of CoMFA, CoMSIA and [(SW) kNN MFA].

Statistics	CoMFA	CoMSIA	[(SW) kNN MFA]
PCs	4	6	3
r^2	0.817	0.822	0.8413
q^2	0.632	0.577	0.6278
pred_r^2	–	–	0.5078
SEE	0.152	0.150	0.1852
F value	44.177	38.623	25.434
P value	0.0	0.0	–
Field contribution			
Steric	0.524	0. 211	S_458 (0.34)
Electrostatic	0.476	0.289	E_472 (0.48)
			E_284 (0.18)
Hydrophobicity	–	0.332	–
H bond acceptor	–	0.123	–
H bond donor	–	0.045	–

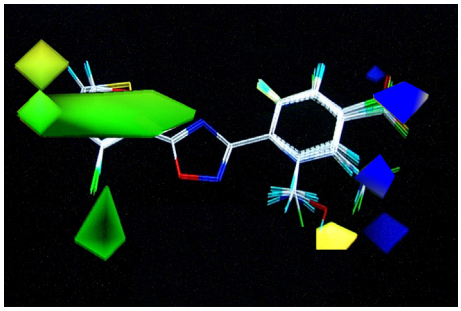

Figure 3 CoMFA contour plots for steric and electrostatic regions. Green counters indicate the bulky group region, whereas the yellow counter indicates the region where bulky groups are not required. Blue counters indicate the region needed for electronegative contribution, whereas red counters indicate the region where electropositive contribution is required.

Table 3 The comparison of PLS statistics results of 3D QSAR Models of CoMFA, CoMSIA and [(SW) kNN MFA] with Gold doc score.

Comp. No.	Actual pIC_{50}	3D QSAR						Docking
		CoMFA Predicted pIC_{50}	CoMFA Residual	CoMSIA Predicted pIC_{50}	CoMSIA Residual	[(SW) kNN MFA] Predicted pIC_{50}	[(SW) kNN MFA] Residual	Gold Score
1d	2.9172	2.7606	0.1566	2.8591	0.0581	2.9797	−0.0625	50.7710
4a	2.7520	2.5558	0.1962	2.7075	0.0445	2.797	−0.045	48.3245
4b	2.5496	2.4697	0.0799	2.6115	−0.0619	2.809	−0.2594	47.1051
4c	3.0506	2.7496	0.301	2.8744	0.1762	3.1098	−0.0592	51.6726
4d	2.3799	2.3634	0.0165	2.3601	0.0198	2.1979	0.182	52.8594
4e	2.4365	2.6706	−0.2341	2.5715	−0.135	2.4972	−0.0607	50.8465
4g	3.0456	3.0214	0.0242	2.9884	0.0572	3.0809	−0.0353	50.3570
4h	2.8508	2.8565	−0.0057	2.9465	−0.0957	2.6909	0.1599	50.2127
4i	3.0315	3.0237	0.0078	3.0253	0.0062	3.2002	−0.1687	50.3041
4j	3.0406	3.0195	0.0211	2.9422	0.0984	3.0763	−0.0357	56.3197
4k	2.8416	2.8221	0.0195	2.9434	−0.1018	2.8902	−0.0486	50.2944
4l	2.7986	2.6402	0.1584	2.8036	−0.005	2.6999	0.0987	51.4326
4m	3.0362	3.0395	−0.0033	3.0703	−0.0341	3.197	−0.1608	49.3034
4n	3.1249	2.9534	0.1715	2.9355	0.1894	3.1213	0.0036	50.9304
4o	2.4789	2.6177	−0.1388	2.7238	−0.2449	2.2991	0.1798	50.9680
4v	2.7055	2.7565	−0.051	2.7137	−0.0082	2.5701	0.1354	50.2641
10a	2.9666	2.8706	0.096	2.7724	0.1942	2.8731	0.0935	49.3839
10b	2.7595	2.7674	−0.0079	2.7528	0.0067	2.6891	0.0704	49.6805
10c	1.7595	1.7815	−0.022	1.8098	−0.0503	1.7897	−0.0302	47.3030
10d	2.6968	2.8924	−0.1956	2.9267	−0.2299	2.4789	0.2179	50.2051
10e	3.2840	2.9656	0.3184	2.9098	0.3742	3.4076	−0.1236	51.2655
10f	2.7932	2.9397	−0.1465	2.8538	−0.0606	2.6762	0.117	49.3028
10g	3.2147	3.1878	0.0269	3.0555	0.1592	3.1237	0.091	49.2035
10h	2.9547	2.8354	0.1193	2.8344	0.1203	3.17979	−0.22509	49.8395
11a	2.7696	2.8163	−0.0467	2.9568	−0.1872	2.7349	0.0347	50.2123
11b	2.6198	2.7063	−0.0865	2.6654	−0.0456	2.8732	−0.2534	49.4238
11c	2.5086	2.5936	−0.085	2.4908	0.0178	2.5021	0.0065	45.9621
11d	2.3468	2.4373	−0.0905	2.3735	−0.0267	2.4012	−0.0544	47.8606
11e	2.9580	2.8504	0.1076	2.8142	0.1438	3.2233	−0.2653	49.3778
11f	3.0268	3.0047	0.0221	3.1097	−0.0829	3.0331	−0.0063	50.8911
11g	2.6575	2.6257	0.0318	2.4664	0.1911	2.7183	−0.0608	48.1746
11h	2.5376	2.6775	−0.1399	2.4605	0.0771	2.5809	−0.0433	47.6375

The final model was developed with an optimum number of components (N) yielding the highest crossvalidated correlation coefficient (q^2) to avoid overfitted 3D QSARs. The other statistical parameters included: number of components, the correlation coefficient (r), coefficient of determination (r^2), r^2 for external test set (pred_r^2), covariance ration (F) and standard error (r^2 se).

3.1. CoMFA results

3D-QSAR models were built by template based alignment method in SYBYL Molecular design Software (Fig. 1).

For the selected CoMFA model, the cross-validated r^2 (q^2) value was 0.632 with four principal components. The non-cross-validated r^2 value was 0.817 with a standard error of estimate 0.152 and a covariance ratio (F) of 44.177 (significant at 99% level) (Table 2).

In CoMFA model, the steric parameter contributes 52.4%, while the electrostatic parameter accounts for 47.6%. Contributions of steric and electrostatic fields are shown in Fig. 3. The correlation between experimental and predicted activity for both training and test sets of compounds is shown in Table 3 and represented graphically in Fig. 4, respectively. These results authenticate the good prediction ability of the generated 3D QSAR model. The model summary dialog box, showed the relative positions of the local fields around aligned molecules that were important for activity variation in the model (Fig. 3). Greater values of "Bio-Activity Measurement" are correlated with more bulky near green, less bulky

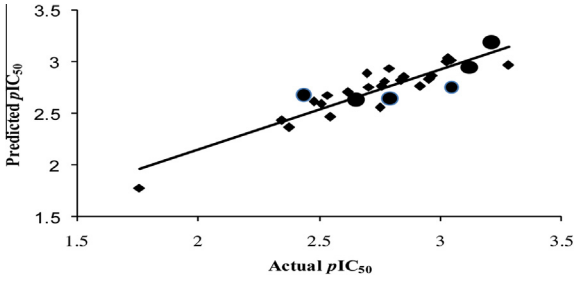

Figure 4 Correlation between the experimental and predicted activities of the developed CoMFA model. (♦ Represent training data set, ● Represent test data set).

near yellow, more electro-negative near blue and less electro-negative or electro-positive charge near red. A large green counter near the 5th -position of the substituted furan ring (Ar_1 substitution) of 1,2,4-oxadiazole ring, indicates that the bulky substitution favors the activity. Thus the presence of a bulky substitution like bromine at 3rd position substitution (compound 10a) encourages the activity. Naturally, presence of chlorine atom at 3rd position in compound 10b is more bulky than unsubstituted in compound 10c thus compound 10b is more active than compound 10c. Activity may further be enhanced by replacing the chlorine atom with bromine (i.e., compound 10b and 10a, respectively) due to more bulkiness of bromine as compared to chlorine. Less bulky group substitution demonstrated with a yellow contour has no significant contribution to activity. Similarly, a blue contour near the 3rd position of the substituted oxadiazole ring (Ar_2), indicates that substitution with electronegative groups like CN, F, Cl increases the activity. Thus the presence of a trifluoromethyl group in compounds (1d, 4i, 4k and 10g) rendered them more active then compounds containing chlorine atoms (4a, 4h, 4l and 10f), respectively. Electropositive substitution demonstrated with a red contour has no contribution to activity.

3.2. CoMSIA results

For the selected CoMSIA model, the cross-validated r^2 (q^2) value of the training set was 0.577 with the optimum number of components (N) six. The regression coefficient (r^2) value was 0.822 with standard error of estimation (SEE) 0.150 and covariance ratio (F) of 38.623 (significant at 99% level) (Table 2). The correlation between experimental activity (EA) and predicted activity (PA) is shown in Fig. 5 and reported in Table 3. The CoMSIA model was externally validated with the test set of compounds. These results demonstrated that the obtained CoMSIA model has good self-consistency ($r^2 > 0.8$) and good prediction ability ($q^2 > 0.5$). The data clearly illustrate the steric, electrostatic, hydrogen-bond donor, hydrogen-bond acceptor and hydrophobic field interaction in the CoMSIA model. In the CoMSIA model, the contributions of the steric, electrostatic, hydrophobic, hydrogen-bond acceptor and hydrogen bond donor fields were 21.1%, 28.9%, 33.2%, 12.3%, and 4.5%, respectively (Table 2) and are represented graphically in Figs. 6 and 7. Similar to CoMFA the presence of a green contour near the fifth position substituted oxadiazole derivatives (Ar_1) indicated that the

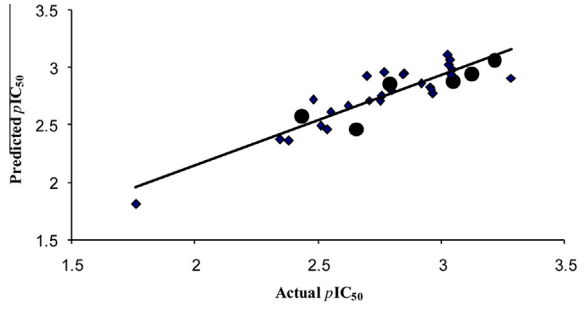

Figure 5 Correlation between the experimental and predicted activities of the developed CoMSIA model. (♦ Represent training data set, ● Represent test data set).

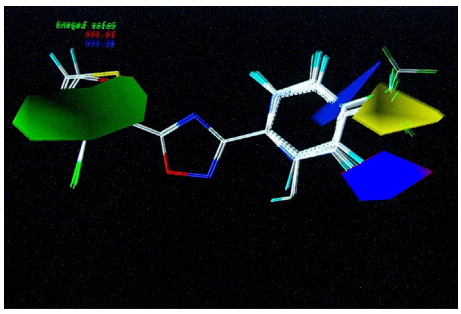

Figure 6 CoMSIA contour plots for Steric and Electrostatic regions. Green counters indicate the bulky group region, whereas yellow counters indicate the region where less bulky groups are required. Blue counters indicate the region needed electronegative contribution.

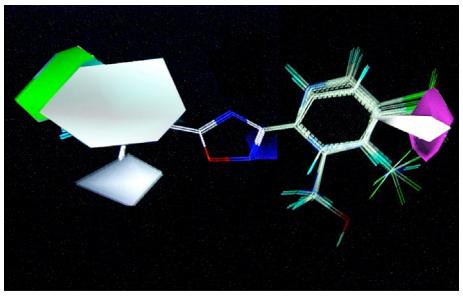

Figure 7 CoMSIA contour plots for hydrophobic, hydrogen bond donor and hydrogen bond acceptor fields region. The white contour near suggest that hydrophobic groups will increase activity and cyan contour decrease the activity. The purple and orange contour for both hydrogen-bond donor favor and not favor respectively in biological activity are absent. Similarly contour for both hydrogen bond acceptor favor and disfavor are showed by magenta contour and green contour respectively.

bulky groups at this position increased activity. The yellow contour above the third position of the substituted phenyl system (Ar_2) indicates that bulky substituents at this position decrease anticancer activity and small group substitution or unsubstitution adds to the biological activity. The blue contour near the third position of the substituted phenyl ring (Ar_2) indicates that the biological activity will increase by an electronegative group at the aforementioned positions (i.e., presence of CF_3 in compounds 1d, 4i, 4k and 10g) (Fig. 6). In the hydrophobic contour plots (Fig. 7) the white contour near 3rd and 5th positions of the substituted (Ar_2 and Ar_1, respectively) oxadiazole ring system suggests that hydrophobic groups like long chain alkyls at this position will add to activity, while a diminutive cyan color indicates no significant contribution of hydrophobic disfavor in biological activity. The purple counter near the 5th position of the substituted (Ar_2) system suggests that the hydrogen-bond donor favored activity and orange contours for hydrogen-bond donor not favored are absent showing no contribution in biological activity. Similarly contours for both hydrogen bond acceptors that were favored and disfavored (magenta contour and green contour respectively) showed no significant contribution in anticancer activity.

Please cite this article in press as: Vaidya, A. et al., CoMFA, CoMSIA, kNN MFA and docking studies of 1,2,4-oxadiazole derivatives as potent caspase-3 activators. Arabian Journal of Chemistry (2014), http://dx.doi.org/10.1016/j.arabjc.2014.05.034

3.3. [(SW) kNN MFA] results

In the [(SW) kNN MFA] method the results of uni-column statistics are summarized in Table 4, which show that the test is interpolative. The final model was selected on the basis of statistical parameters of the models. Finally, the model with good internal and external predictive abilities was selected and is shown in Table 2.

For the selected [(SW) kNN MFA] model, the cross-validated r^2 (q^2) value of the training set was 0.6278 with three principal components. The non-cross-validated r^2 value was 0.8413 with a standard error of estimate of 0.1852 and a covariance ratio (F) of 25.434 (significant at 99% level). The predictive ability of the model was also confirmed by external pred_r^2 having the value 0.5078 (Table 2).

In kNN MFA model, the steric parameter contributes 34%, while the electrostatic parameter accounts for 66%. Contributions of steric and electrostatic fields are shown in the contribution chart (Fig. 8). The correlations between experimental and predicted activity for both training and test set of compounds are shown in Table 3 and represented graphically in Fig. 9 respectively, authenticate the good prediction ability of the generated 3D QSAR model. The model summary dialog box, showed the relative positions of both steric (green counter) and electrostatic regions (blue counter) around aligned molecules that were important for activity variation in the model (Fig. 10). Like CoMFA and CoMSIA, the green counter near the 5th position of the substituted furan ring of

Table 4 Unicolumn statistics of the training and test set.

	Average	Max.	Min.
Training set	2.7943	3.2840	1.7595
Test size	2.7324	3.1249	2.4365

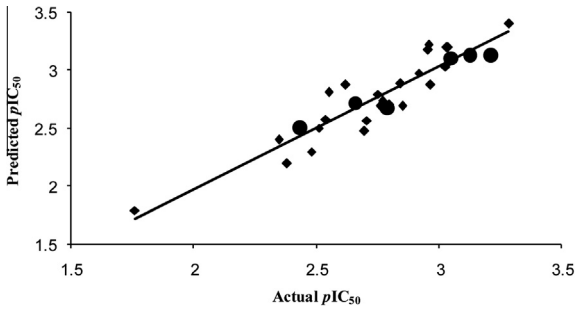

Figure 9 Correlation between the experimental and predicted activities of the developed 3D QSAR by [(SW) kNN MFA] model. (♦ Represent training data set, ● Represent test data set).

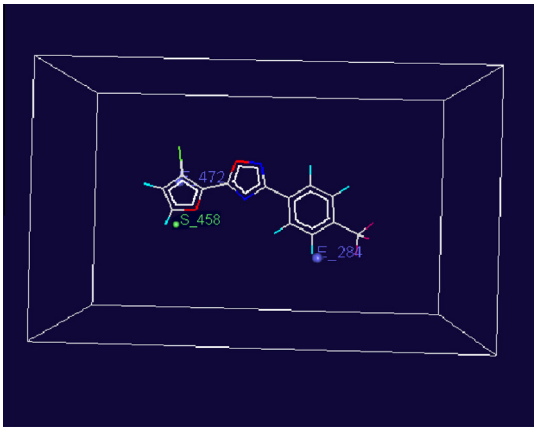

Figure 10 kNN MFA contour plots for steric and electrostatic regions. Green counters (S) indicate the steric region, whereas blue counters (E) indicate region where electrostatic contribution are required.

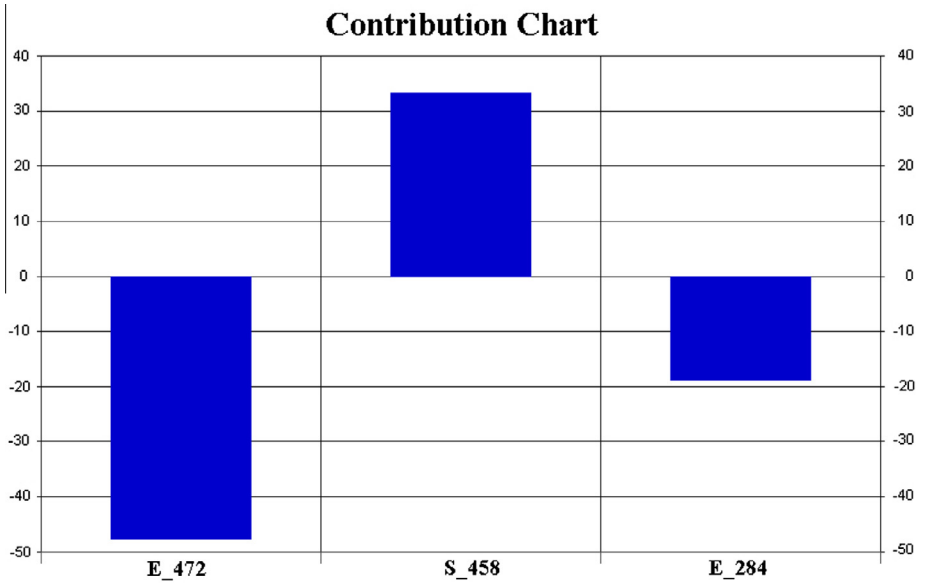

Figure 8 Contribution of steric and electrostatic fields generated in 3D QSAR by [(SW) kNN MFA] model.

1,2,4-oxadiazole derivatives indicates that biological activity can be improved by introducing a bulky group. Presence of a blue counter near the 3rd and 5th positions of the substituted furan and phenyl rings respectively of 1,2,4-oxadiazole derivatives favors the presence of an electronegative group at aforementioned positions.

Thus on the basis of 3D QSAR including CoMFA, CoMSIA and [(SW) kNN MFA] analyses the presence of bulky groups such as ethoxy and phenoxy at the 5th position of the-substituted furan ring of 1,2,4-oxadiazole derivatives and substitution of electronegative groups including di-fluoro and trimethy fluoro at 3-substituted phenyl ring of 1,2,4-oxadiazole derivatives are conducive to caspase-3 activating activity.

3.4. Docking results

It is well-reported that the anticancer mechanism of 3-Aryl-5-aryl-1,2,4-oxadiazoles is due to caspase-3 activation. Therefore, a docking study could offer understanding the protein–activator interactions and the structural features of the active site of the protein.

All 1,2,4-oxadiazoles derivatives were docked into the binding site of caspase-3 and the energy scores of the activators are also shown in Table 3, where precise correlations could be found between docking scores and pIC_{50} values.

A complete overview of Gold docking is presented in Figs. 11 and 12. Correlation between the docking score and experimental activity is shown graphically in Fig. 13. It vividly represents the interaction model of the most potent activator 10e with caspase-3. Docking studies showed that activator 10e is suitably situated at the binding site and there are various interactions between it and the binding region of the enzyme. The oxadiazole ring binds to the Caspase hinge region through three key hydrogen bond interactions: (1) between the NH of Cys205 and the O of the oxadiazole ring (2) between the NH of Gly238 and the O of the oxadiazole ring (3) between the NH of Cys205 and the N of the oxadiazole ring. Similarly the 5th position of the substituted furan ring also forms hydrogen bonding between the NH of Gly238 and the O of the furan ring. The hydrogen bonding distances observed were 2.319 Å (O_ _ _ H–NH– Cys205), 2.532 Å (O_ _ _ H–NH– Gly238),

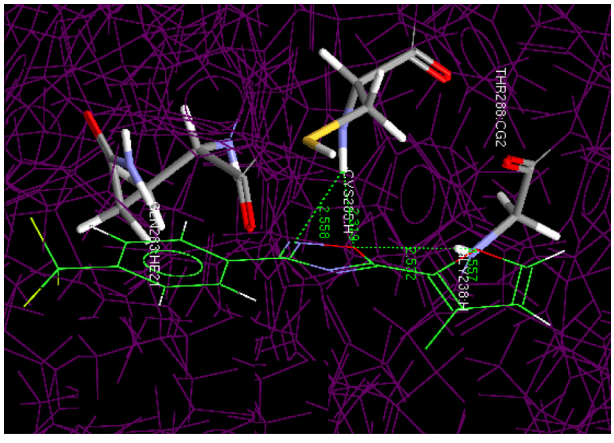

Figure 11 Overlay of docked highest potent oxadiazole compound (10e) at the active site of 1RE1 produced using the Gold program.

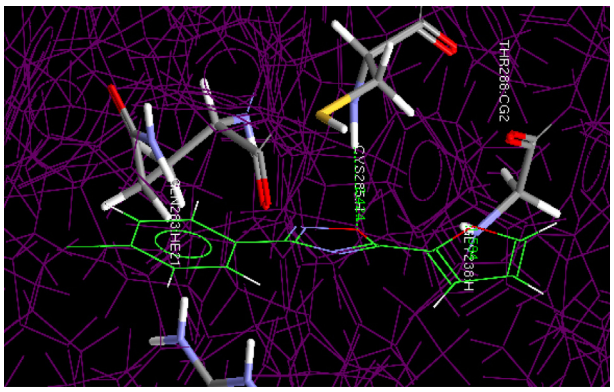

Figure 12 Overlay of docked least potent oxadiazole compound (10c) at the active site of 1RE1 produced using the Gold program.

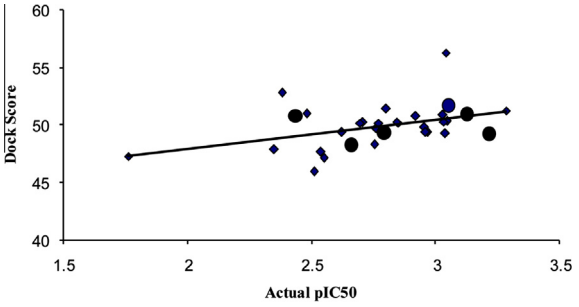

Figure 13 Correlation between the experimental activity and dock score in Gold docking. (♦ Represent training data set, ● Represent test data set).

2.558 Å (N_ _ _ H–NH– Cys205) and 1.557 Å between the O of the furan ring and NH of Gly238 (O_ _ _ H–NH– Gly238).

Fig. 12 shows the docking mode of the least active oxadiazole derivative compound 10c at the docking pocket. Similar to compound 10e, compound 10c was also docked at the same binding pockets having Cys205 and Gly238 amino acid residues. Results show that the O atom of the oxadiazole ring forms a conservative hydrogen bond with Cys205 residue (O_ _ _ H-NH-Cys205) having 2.414 Å bond distance. O atom of the furan ring substituted at the 5th position of oxadiazole (Ar_1) also forms hydrogen bonding with NH of Gly238 (O_ _ _ H-NH-Gly238) with 1.594 Å bond length. The docking results reported in Table 3, reveal that hydrogen bonding may be responsible for activity, which may be further increased on adding high electronegative substitutions.

Results of CoMFA, CoMSIA and [(SW) kNN MFA] methods, clearly show that the presence of an additional electronegative substitution at the 3rd position (Ar_2 substitution) of 1,2,4-oxadiazole enhances biological activity. The presence of electronegative substitution at the 3rd position is responsible for biological activity and related data were further confirmed by docking results. Docking results clearly reveal that the presence of an additional electronegative group at 3rd position substitution (10e) forms more hydrogen bonds with their surrounding amino acid residues (3 hydrogen bonds with Cys205 and Gly238) and thus possesses improved biological activity in comparison to compounds that possess less number

Please cite this article in press as: Vaidya, A. et al., CoMFA, CoMSIA, kNN MFA and docking studies of 1,2,4-oxadiazole derivatives as potent caspase-3 activators. Arabian Journal of Chemistry (2014), http://dx.doi.org/10.1016/j.arabjc.2014.05.034

of electronegative substitutions (10c) at the aformentioned positions. These data justify the results of 3D QSAR and docking results and also confirm the utility of this hybrid technique.

4. Conclusions

In the present study, 3D-QSAR and molecular docking studies were performed on a series of caspase-3 activators. The 3D-QSAR studies were done using CoMFA, CoMSIA and [(SW) kNN MFA] methods, which gained some insight into the key structural factors affecting the bioactivity of these inhibitors. The results of 3D-QSAR strongly suggest the presence of bulky group substitution near the 5th position of furan ring (Ar_1 substitution) whereas the presence of an electronegative group near the third position of substituted phenyl ring (Ar_2) is also conducive for the activity. Docking studies were performed using Gold docking programs to obtain the bioactive conformations for the whole dataset. In Gold docking the activator with the highest potency (compound 10e) forms three hydrogen bonds with residues of hinge region amino acids Cys205 and Gly238. In spite of this, compounds having least experimental activity (10c) show only two hydrogen bonds.

Acknowledgments

We would like to thank the Director, IICT Hyderabad, India, for providing access to computational resources and for their valuable help during the modeling studies.

References

Cai, S.X., Zhang, H.Z., Guastella, J., Drew, J., Yang, W., Weber, E., 2001. Bioorg. Med. Chem. Lett. 11, 39.
Carson, D.A., Lois, A., 1995. Lancet 346, 1009–1011.
Dutchowicz, P.R., Fernandez, M., Carballero, J., Castro, E.A., Fernandez, F.M., 2006. Bioorg. Med. Chem. 14, 5876s.
Jain, A.K., Veerasamy, R., Vaidya, A., Mourya, V., Agrawal, R.K., 2010. Med. Chem. Res. 19, 1191.
Kemnitzer, W., Kuemmerle, J., Zhang, H.Z., Kaisbhatla, S., Tseng, B., Drew, J., Cai, S.X., 2009. Bioorg. Med. Chem. Lett. 19, 4410.
Leonard, J.T., Roy, K., 2006. Bioorg. Med. Chem. 14, 1039.
Marques, C.A., Keil, U., Bonert, A., Steiner, B., Haass, C., Muller, W.E., Eckert, A., 2003. J. Biol. Chem. 278, 28294.
Mohr, A., Zwacka, R.M., 2007. Cell. Biol. Int. 31, 526.
Prashanthakumar, B.R., Nanjan, M.J., 2009. Med. Chem. Res. 19, 1000.
Ravichandran, V., Agrawal, R.K., 2007. Bioorg. Med. Chem. Lett. 17, 2197.
Ravichandran, V., Jain, P.K., Mourya, V.K., Agrawal, R.K., 2007. Med. Chem. Res. 16, 342.
Ravichandran, V., Sankar, S., Agrawal, R.K., 2008. Med. Chem. Res. 17, 1.
Salvesen, G.S., Dixit, V.M., 1997. Cell 91, 443.
Silva, S.R.D., Bacchi, M.M., Bacchi, C.E., Oliveira, D.E.D., 2007. Am. J. Clin. Pathol. 128, 794.
Sohn, E.J., Li, H., Reidy, K., Beers, L.F., Christensen, B.L., Lee, S.B., 2010. Cancer Res. 70, 115.
Suk, O.Y., Young, K.H., Jin, J.S., Young, P.K., Young, K.S., Jung, L.H., Ok, L.E., Seok, A.K., Hoon, K.S., 2009. Chin. Sci. Bull. 54, 387.
SYBYL [computer program], version 6.9. St. Louis (MO): Tripose Associates, USA.
Syed, F.M., Hahn, H.S., Odley, A., Guo, Y., Vallejo, J.G., Lynch, R.A., Mann, D.L., Bolli, R., Dorn, G.W., 2005. Circ. Res. 96, 1103.
Thornberry, N.A., 1998. Chem. Biol. 5, 97.
Thun, M.J., Henley, S.J., Burns, D., Jemal, A., Shanks, T.G., 2006. J. Natl. Cancer Inst. 98, 691.
Vaidya, A., Jain, A.K., Kumar, P., Kashaw, S.K., Agrawal, R.K., 2011. J. Enzyme Inhib. Med. Chem. 26, 854.
V-Life Molecular Design Suite 3.0, VLife Sciences Technologies Pvt. Ltd; Baner Road: Pune, Maharashtra, India. www.Vlifesciences.com.
Zhang, H.Z., Kashibhatla, S., Guastella, J., Drew, J., Tseng, B., Cai, S.X., 2003. Bioconjugate Chem. 14, 458.
Zhang, H.Z., Kaisbhatla, S., Kuemmerle, J., Kemnitzer, W., Mason, K.O., Qui, L., Grundy, C.C., Tseng, B., Drew, J., Cai, S.X., 2005a. J. Med. Chem. 48, 5215.
Zhang, H.Z., Shailaja, K., Jared, K., William, K., Kristin, O.M., Ling, Q., Candace, C.G., Ben, T., John, D., Sui, X.C., 2005b. J. Med. Chem. 48, 5215.